

Recent progress of the Liège Intranuclear Cascade Model¹

J. Cugnon^{*}, Th. Aoust^{†*}, P. Henrotte^{*}, A. Boudard^{**}, S. Leray^{**} and C. Volant^{**}

^{*}University of Liège, Physics Department B5, allée du 6 Août 17, Bât B5, B-4000 Liège 1, Belgium

[†]SCK-CEN, Boeretang 200, B-2400 Mol, Belgium

^{**}DAPNIA/SPhN, CEA/Saclay, F-91191 Gif-sur-Yvette Cedex, France

Abstract. The Liège intranuclear cascade model has been shown by the HINDAS collaboration to successfully describe spallation reaction data in the 200 MeV to 2 GeV range. We report here on the recent progress obtained afterwards. They bear on the behaviour of the model at low energy, on the introduction of an energy and isospin dependence of the mean field, on the improvement of pion production mechanism and on the inclusion of composite production in the cascade.

INTRODUCTION

The Liège Intranuclear Cascade (INCL) model has recently evolved, during the HINDAS collaboration, to a numerical code INCL4, which, without any parameter tuning, is able to give good results for an impressive set of data concerning spallation reactions in the ~ 200 MeV to 2 GeV range of incident energies [1, 2]. These data includes total reaction cross-sections, neutron and proton double differential cross-sections, particle multiplicities, residue mass and charge spectra, isotopic distributions and residue recoil energy distributions, for proton-induced as well as deuteron-induced reactions.

Here, we shortly describe the INCL4 model and report on the progress obtained since the end of the HINDAS collaboration.

THE INCL4 MODEL

The INCL4 model provides with a time-like picture of the collision mechanism, made of a succession of binary collisions, particle decays or refraction/reflexion on the surface, well separated in space-time. Elementary collisions are decided on closest distance of approach basis and final states are determined at random according to experimental data, subject possibly to statistical Pauli blockers.

Typical features of INCL4 (compared to previous versions) are: (1) a smooth nuclear surface (2) a consistent implementation of the Pauli blocking: collisions are allowed if they passed the test for the Pauli blockers but

also if the original Fermi sphere (below the Fermi level) is excited (3) spectators are moving but do not collide with each other (4) pion dynamics is improved (5) extension to light clusters as incident particles (6) prediction of the angular momentum of the target remnant.

The success of the INCL4 code comes from the introduction of a diffuse surface and from an improved treatment of the Pauli principle, as has been shown within the HINDAS collaboration, and especially, in our opinion, from the self-consistent determination of the stopping time, i.e. the time at which the cascade is stopped and the evaporation code is started. This feature seems to free the model from the introduction of a so-called pre-equilibrium module.

THE LOW-ENERGY BEHAVIOUR

The condition for the validity of the independent collision picture is, roughly speaking, expressed by

$$\lambda_B \ll r_0 \ll d, \quad (1)$$

where λ_B is the de Broglie wavelength for the nucleon-nucleon relative motion, r_0 is the range of nuclear force and d the average distance between neighbouring target nucleons. The second inequality is (barely) fulfilled in the nuclear case. The first inequality is certainly not fulfilled, even for the first collision, when the incident energy is less than 100 MeV. It is the reason why so-called pre-equilibrium models are generally used in this energy range, although it was pointed out from time to time that INC models does not generate crazy results. But, the validity of the INC model, as far as results are concerned, had never been truly investigated, before the work of Ref. [3]. In this work, the validity of the INCL

¹ Invited talk to the ND2004 Conference, Santa Fe, Sept. 2004

model is tested by boldly comparing its predictions with experimental data. However, a little bit more flexibility is introduced compared to Ref. [1]: first the reaction cross-section is not normalised on the model itself, but on the experimental data, and second, the Pauli principle is made more strict. In ref. [3], it is shown that results are better with a strict Pauli blocking instead of the usual statistical implementation. Even better results are obtained by combining a strict Pauli blocking for the first collision with a statistical blocking for the subsequent collisions. A typical result is shown in Fig.1. Two important results come out of the work of Ref. [3]. First, above 40 MeV, there is little dependence of the cross-sections upon the detailed properties (structure) of the target. They vary smoothly with target mass and incident energy. As a result, the agreement displayed in Fig.1 is indicative of the whole domain of target mass number above (^{27}Al) and of incident energy between ~ 40 to 200 MeV. Second, the results of the INCL model are competing reasonably well (in view of the simplicity of the model) with current “pre-equilibrium” models, traditionally used in this energy range. Fig.1 illustrates this point. We remind that these models try to account for the quantum motion of the nucleons. Obviously, the effects of the latter is not evident. Let us stress that our comment applies to incoherent nucleon production. Coherent excitation of low-lying states as well as production of clusters are more sensitive to structure details.

THE NUCLEAR MEAN FIELD

In INC models, nucleons are supposed to experience a nuclear mean field, that is represented by a potential well of fixed depth, generally the same for protons and neutrons. This is not consistent with the phenomenology of the optical-model potential [6]. The real part of the latter depends upon the isospin of the nucleons (T_3) and upon their energy (E). Roughly speaking, the depth of the potential is linearly decreasing with the nucleon energy until the latter reaches $E_0 \sim 200$ MeV, beyond which it basically vanishes. We introduced both an isospin- and energy-dependent nuclear potential in INCL. The depths of the potentials $V_0^i(E)$, $i = n, p$ are given by

$$\begin{aligned} V_0^i(E) &= V_0^i - \alpha_i(E - E_F^i), \text{ for } E < E_0 \\ &= 0, \text{ for } E > E_0, \end{aligned} \quad (2)$$

where E is the total energy

$$E = \frac{\hbar^2 k^2}{2M} + V_0^i(E). \quad (3)$$

The Fermi energies E_F^i are then given by

$$E_F^i = \frac{\hbar^2 k_F^{i,2}}{2M} + V_0^i, \quad (4)$$

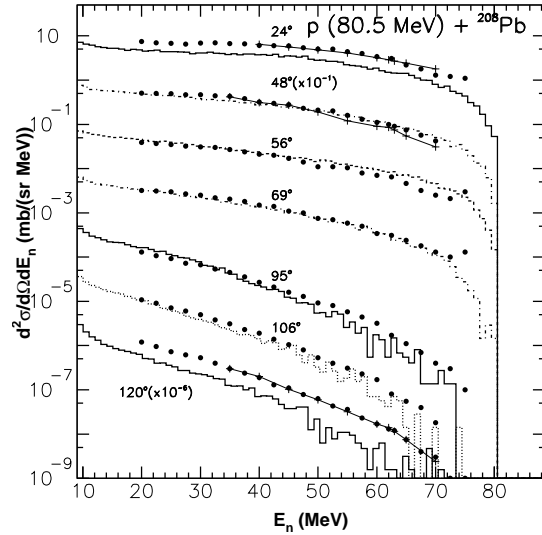


FIGURE 1. Double differential neutron cross-section for $p + ^{208}Pb$ reactions at 80.5 MeV. Data (dots) are taken from ref. [4] (coherent excitation peaks to some low-lying states are not shown). Data are compared with the predictions of the INCL model (histograms) and with the ones of the Multi-Step Direct (MSD) model of ref. [5] (continuous lines, as quoted in ref. [4]). Adapted from Ref. [3].

TABLE 1. Multiplicities per primary reaction obtained in proton-induced reactions on ^{208}Pb at 800 MeV. Comparison of the results for various types of nuclear mean field: standard (2d column), isospin-dependent (3d column), isospin- and energy-dependent (4th column). Experimental data are from ref. [7].

	Stan- dard	T_3	T_3 & E	Exp
$n, E > 20$ MeV	2.48	2.28	2.21	1.9 ± 0.2
$n, E > 2$ MeV	9.30	9.26	9.23	10.4 ± 1.4
$p, E > 20$ MeV	2.07	2.20	2.18	
$p, E > 2$ MeV	2.55	2.70	2.65	

The Fermi momenta are determined by the central density of the nucleus and the N/Z ratio. Identifying $-E_F^i$ as the separation energy for type- i nucleons totally determines the constants V_0^i . Parameters α_i are taken from Ref. [6]

The effect of introducing these phenomenological potentials are shown in Table 1 and Fig.2. The main effect is due to the isospin-dependence: less neutrons and more protons are emitted in the cascade stage. This is due to the average binding energy, which has increased for neutrons and decreased for protons. The excitation energy at the end of the cascade stage has increased. As a result, the number of emitted neutrons has increased. The shape

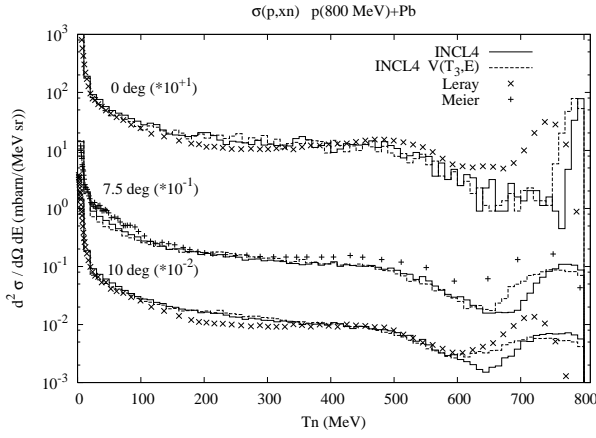


FIGURE 2. Double differential neutron cross-section for $p + {}^{208}\text{Pb}$ reactions at 800 MeV. Comparison between standard INCL4 predictions (full histograms) and after introduction of an isospin and energy-dependent mean field (dashed histograms). Data are taken from refs. [7, 8]. The data of ref. [7] are not corrected for target thickness.

of the particle spectra has not changed very much except in the vicinity of the quasi-elastic peak (see Fig.2). Roughly speaking, the neutron peak has shifted toward larger energy loss, by about 20 MeV, coming closer to the experimental results. Here also, the effect is mainly due to the isospin dependence and can be explained on the basis of average binding energy for neutrons and protons. This also explains why the proton quasi-elastic peak is basically not shifted.

PION DYNAMICS

We also investigated the effect of the average potential for pions (in the standard INCL code, this potential is set to 0). This is a rather tricky question, as the pion optical-model potential is dominated by resonant absorption [9]. Causality in quantum mechanics forces the real potential to be largely dispersive: it assumes large values in the nuclear volume, which may vary rapidly with the energy. That is why sometimes even the sign of the potential is not unambiguously determined by the fits. In the nuclear surface (where absorption is reduced) the real potential is rather shallow and slightly attractive. For a first simple investigation of the global effect of pion potential, we introduced an energy-independent (but isospin-dependent) square-well potential for the pions. Results are shown in Fig.3 for production of positive pions in $p + {}^{208}\text{Pb}$ collisions at 730 MeV. Considering also the production of negative pions (not shown), this analysis indicates that the best results are obtained for repulsive pion potentials with a strength of ~ 60 MeV for π^+ 's and ~ 25 MeV for

π^- 's², respectively. The π^- yield is only overestimated by 10 percent. This undoubtedly improves our predictions for pion production [1]. However, pion production is a complex mechanism and one has to keep in mind that many other medium effects, that are not taken into account, can influence the pion yield.

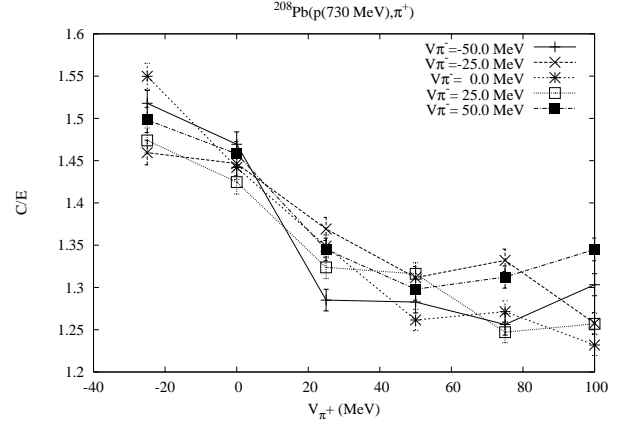


FIGURE 3. Ratio between calculated and experimental [10] total π^+ -production cross-section in $p + {}^{208}\text{Pb}$ collisions at 730 MeV. Calculations has been done with the INCL model for various depths of the pion potential.

PRODUCTION OF CLUSTERS

One nice feature of INC models with a pre-equilibrium module is the fact that they can accommodate the production of light clusters with energy larger than in the evaporation. We have also implemented a relatively simple model in INCL4 which allows the production of clusters in the cascade stage. When a nucleon arrives at the surface and is going to be emitted, it is checked whether it can drag with him one or several nucleons which are sufficiently close to each other in phase space. The following clusters (d , t , ${}^3\text{He}$ and ${}^4\text{He}$) are considered up to now, but the method could be extended to heavier clusters. If a large cluster has been built, it is emitted if the energy of the cluster is sufficient and if it succeeds the test for transmission through the relevant Coulomb barrier. If not, the smaller clusters inside the original one are tested for emission, and so on. We refer to Ref. [11] for more detail. In simple words, this model is a kind of surface coalescence model based on the dynamic phase space distribution in the surface region at any time. It is different from the usual coalescence model: as a matter of fact, it does violate the scaling laws of this model.

Typical results are shown in Table 2 and Fig.4. The latter shows the triton cross-section in $p + \text{Au}$ collisions at

² Taking the mean value for π^0 's.

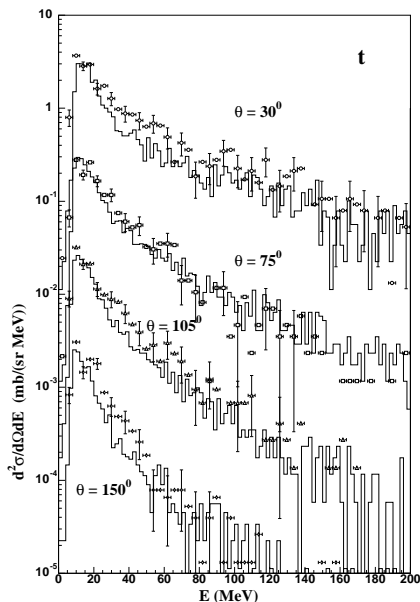


FIGURE 4. Comparison of the results of INCL4 model, supplemented with the cluster emission model outlined above and coupled to the GEM evaporation code, for triton production in the $p + Au$ system at 2.5 GeV (histograms) with the experimental data (symbols) of Ref. [12]. Cross-sections are given in absolute values for the smallest angle. They are multiplied by 10^{-1} , 10^{-2} , etc, for the other angles, in increasing order.

TABLE 2. Multiplicities per primary reaction obtained in proton-induced reactions on ^{208}Pb at 1.2 GeV. Experimental data are from ref. [7].

	without clusters	with clusters	Exp
n , (casc)	4.13	3.52	
n , (tot)	14.61	14.27	
n , (free+bound)	15.93	16.52	
n , $E > 20$ MeV	3.17	2.67	2.7 ± 0.3

2.5 GeV. The agreement is rather satisfactory. Note that the energy spectrum extends much outside the evaporation domain. It is interesting to look at multiplicities. The introduction of the cluster formation in the cascade stage reduces the number of neutrons emitted in the cascade stage, as expected. Evaporation is not much affected. However the total number of neutrons (free or hidden inside clusters) is enhanced. The number of neutrons of more than 20 MeV is slightly reduced, with improves our previous calculations. It is also interesting to point out than the ratio of emitted particles remains roughly the same in a large domain of incident energy [11].

CONCLUSION

We reported here on some recent developments of our INCL4 model. We tried to keep on with our general philosophy: introduce as much as known physics as we can, in such a way that it can be treated by the semi-classical INC method without deforming its basic features and without relying on free parameters. We have so introduced an isospin- and energy-dependent nuclear potential for nucleons, which is entirely borrowed from known phenomenology. The effects of this feature affect our results only slightly, but they do improve them.

We attempted also to introduce an isospin-dependent potential for pions. In that case, the phenomenology is less precise than for the nucleon case. However, we have improved our results for pion production with reasonable values of the strength of the potential.

We extended our INCL model to low energy, in a region where the semi-classical approach should fail in principle. We showed that this is not the case, provided a so-called strict implementation of the Pauli principle is introduced. The reasons why the model is still working in this domain are not clear. Presumably, quantum effects in incoherent nucleon emission are cancelling due to the large number of possible channels.

We built a model for accomodating cluster production in the cascade stage. This model is well-founded, but implies two free parameters. We did not attempt to a best fit, but a good description of the cluster production at high energy is obtained with reasonable values of these parameters [11].

All these modifications will be included in the forthcoming version of the INCL code.

REFERENCES

1. Boudard, A., Cugnon, J., Leray, S., and Volant, C., *Phys. Rev. C*, **66**, 044615 (2002).
2. Meulders, J.-P., et al., HINDAS final report, Tech. rep., European Union (2005).
3. Cugnon, J., and Henrotte, P., *Eur. Phys. J. A*, **16**, 393 (2003).
4. Trabandt, M., et al., *Phys. Rev. C*, **39**, 452 (1989).
5. Bonetti, R., Camnasio, D., Colli Milazzo, L., and Hodgson, P. E., *Phys. Rev. C*, **24**, 71 (1981).
6. Hodgson, P. E., *The Nucleon Optical Potential*, World Scientific, 1994.
7. Leray, S., et al., *Phys. Rev. C*, **65**, 044621 (2002).
8. Meier, M. M., et al., *Radiation Eff.*, **96**, 73 (1986).
9. Johnson, M. B., and Satchler, G. R., *Ann. Phys.*, **248**, 134 (1996).
10. Cochran, D. R. F., et al., *Phys. Rev. D*, **6**, 3085 (1972).
11. Boudard, A., Cugnon, J., Leray, S., and Volant, C., *Nucl. Phys. A*, **740**, 195 (2004).
12. Letourneau, A., et al., *Nucl. Phys. A*, **712**, 133 (2002).